

Article

# Response Analysis of Multi-Layered Volcanic Aquifers in Jeju Island to the 2011 M9.0 Tohoku-Oki Earthquake

Byeongho Won <sup>1</sup>, Se-Yeong Hamm <sup>2</sup> , Kue-Young Kim <sup>1</sup> , Kyoochul Ha <sup>1</sup>, Jehyun Shin <sup>1</sup>,  
Seho Hwang <sup>1</sup> and Soo-Hyoung Lee <sup>1,\*</sup>

<sup>1</sup> Korea Institute of Geoscience and Mineral Resources, 124 Gwahang-no, Yuseong-gu, Daejeon 34132, Korea; bhwon@kigam.re.kr (B.W.); kykim@kigam.re.kr (K.-Y.K.); hasife@kigam.re.kr (K.H.); jehyun@kigam.re.kr (J.S.); hwangse@kigam.re.kr (S.H.)

<sup>2</sup> Department of Geological Sciences, Pusan National University, 2 Busandaehak-ro, 63 beon-gil, Geumjeong-gu, Busan 46241, Korea; hsy@pusan.ac.kr

\* Correspondence: rbagio@kigam.re.kr

Received: 7 February 2019; Accepted: 1 May 2019; Published: 5 May 2019



**Abstract:** Seismic waves caused by earthquakes can lead to the movement of fresh groundwater and saltwater in coastal aquifers. The groundwater level, temperature, and electrical conductivity in coastal monitoring wells on the volcanic island of Jeju all responded to the 2011 M 9.0 Tohoku-Oki earthquake. As a result of the earthquake, groundwater temperature and electrical conductivity patterns demonstrated freshwater outflow and saltwater inflow through the monitoring wells in multi-layered coastal aquifers. The seismicity also affected the behavior of ocean tides occurring at depth along the multi-layered coastal aquifers. These observations prove that the use of multi-depth systems for monitoring groundwater level, temperature, and electrical conductivity are more effective than single monitoring systems for understanding the exact behavior of multi-layered aquifers as well as efficiently detecting earthquake-induced or anthropogenic impacts on aquifers in coastal, karstic, or volcanic areas.

**Keywords:** Tohoku-Oki earthquake; multi-layered coastal aquifer; multi-depth system; seismic waves; volcanic island

## 1. Introduction

Groundwater can be affected by numerous factors, including rainfall, earth tides, ocean tides, atmospheric pressure changes, pumping from surrounding wells, and earthquakes. Around the epicenter of an earthquake, coseismic static strain change can trigger a rise or decline in the groundwater level through compression or expansion of aquifers [1–3]. However, other aspects have been reported recently [4]. Far field earthquakes produce hydroseismograms similar to those of seismic waves by expanding and contracting bedrock aquifers and changing the pore pressure in the aquifers. Generally, when seismic waves pass, changes in the pore pressure cause flow into and out of wells from aquifers by dynamic stress (seismic waves). The oscillatory changes in the groundwater level only occur when the aquifer has high enough transmissivity, permeability, etc. [5–8]. Groundwater level oscillation patterns due to seismic impact are directly linked to aquifer properties (transmissivity, storativity, and others) [9–16].

Seismicity also generates chemical changes in groundwater at epicentral and remote sites [17–25]. Changes in temperature and electrical conductivity (EC) have been observed in spring water and groundwater near an epicenter before and after an earthquake [21,26–29]. For instance, significant changes in the salinity and electrical conductivity of two wells were recognized to have been caused by

the mixing of groundwater from different aquifers through fractures that were developed by crustal strain inside the water barrier zone [30]. Another study suggested that the propagation of seismic waves caused changes in temperature via the mixing of upper and lower water, which regained normal temperature when the groundwater reached a normal level after the waves had dissipated [31].

Fluctuations of groundwater levels in coastal aquifers are governed by freshwater-saltwater interactions and oceanic tide effects, together with the complex hydraulic properties of multi-layered systems [32]. In coastal aquifers, EC is used as a general indicator for detecting a freshwater-saltwater boundary as well as the presence of saltwater intrusions [33,34]. However, in coastal areas, seismic waves from earthquakes can destroy the balance between freshwater and saltwater [16]. Multi-layered aquifer systems in volcanic islands often exhibit complex structures and hydraulic properties however, data acquired from specific depths by earthquake monitoring systems only give limited information on the upward or downward movement of groundwater and the groundwater chemistry [35]. Changes to the groundwater chemistry caused by earthquakes can also be utilized as a tool for recognizing the movement of freshwater and saltwater in multi-layered coastal aquifers.

The M 9.0 Tohoku-Oki Earthquake occurred in the region of Honshu, Japan, on 11 March 2011 at 14:46:23 local time (05:46:24 UTC time), and around 30 min later, at 15:15:40, was accompanied by an aftershock of M 7.9. The volcanic island of Jeju is located approximately 1500 km from the two epicenters. Seismic waves were recorded at the Jeju seismological station three minutes after the M 9.0 Tohoku-Oki earthquake; P waves arrived at the station at 14:49:39 local time (05:49:39 UTC) and S waves and Rayleigh waves arrived at 14:52:15 and 14:55:30 local time, respectively.

This study is focused on the response of the multi-layered coastal aquifers in the eastern part of Jeju Island where saltwater intrusion occurs around the freshwater-saltwater boundary [36–38], to the 2011 M 9.0 Tohoku-Oki earthquake, and aims to reveal the hydraulic behavior of the aquifers. For this study, the measurement of groundwater level, EC, and temperature at multiple depths, as well as the geological and geophysical logs, have been used for the monitoring of wells in order to estimate groundwater flow in the multi-layered aquifers.

## 2. Study Area

### 2.1. Monitoring Wells

Located ~140 km south of mainland Korea, Jeju Island has a total area of 1828 km<sup>2</sup>. The island is formed from a dormant shield volcano with a central mountain, Mt. Halla, with an elevation of 1950 m AMSL (above mean sea level). Three monitoring wells (SS-1, SS-2, and SS-3) are located at elevations between 33.8 and 115.5 m AMSL, with depths of 151 to 267 m and depths to water (DTW) of 32.9 to 113.8 m. The three wells are located 1.6 km, 3.2 km, and 5.4 km, away from the coast, respectively (Figure 1, Table 1). The EC and temperature of the multi-depth probe system for well SS-1 were measured at depths of 58 m (S1), 63 m (S2), 68 m (S3), and 111 m (S4) from the land surface, at 30-min intervals [38]. The multi-depth probe system has an EC range of 0–60,000  $\mu\text{S}/\text{cm}$  (accuracy  $\pm 1\%$  full scale, resolution 0.1  $\mu\text{S}/\text{cm}$ ) and a temperature range of  $-5$  to  $50$  °C (accuracy  $\pm 1$  °C, resolution 0.01 °C). At wells SS-1 and SS-3, EC, and temperature were measured using a CTD diver transducer. At well SS-3, the CTD diver transducer was installed at a depth just above the freshwater-saltwater mixing zone. The interval of the groundwater level measurement was once every minute.

**Table 1.** Information about the monitoring wells.

OW *	Elevation (m, AMSL **)	Well Depth (m)	DTW *** (m)	Well Casing Radius (mm)	Screen Zone Below Surface (m)	Distance from Coast (km)
SS-1	33.8	151	32.9	203.2	20–151	1.6
SS-2	70.9	196	69.7	152.4	28–161	3.2
SS-3	115.5	267	113.8	254.0	112–218	5.4

\* OW: Observation well, \*\* above mean sea level (AMSL), \*\*\* DTW: Depth to water.

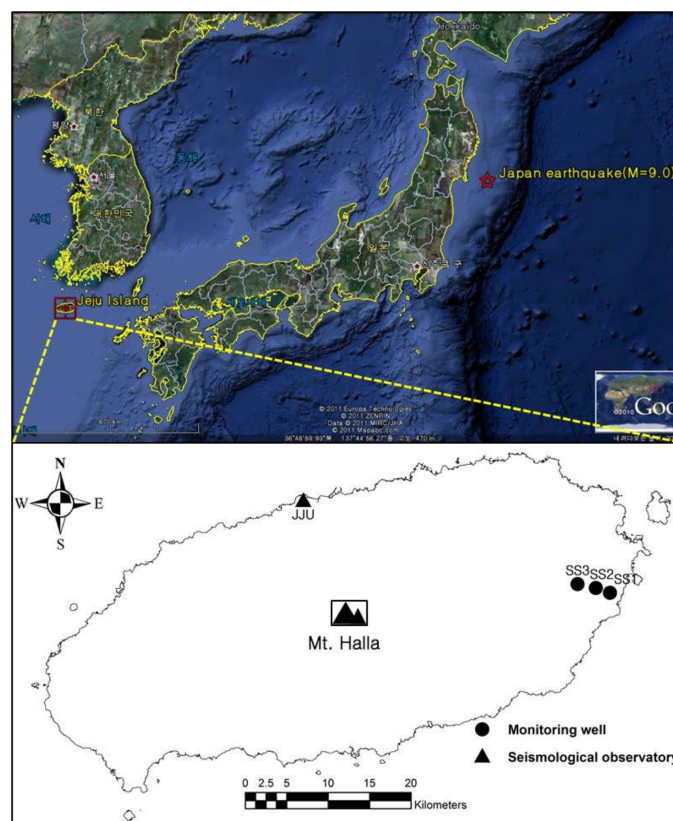


**Figure 1.** Map showing the monitoring wells and the seismological observatory on Jeju Island and the location of the epicenter of the 2011 M 9.0 Tohoku-Oki earthquake.

## 2.2. Geological and Hydrogeological Setting

The geology from bottom to top consists of basement rock (granite and welded tuff), U formation (UF, unconsolidated sediments), Seogwipo formation (SGF, conglomeratic sandstone, sandstone, sandy mudstone, and mudstone containing abundant bio-clastic shells), and lava (basalt and trachyte) [39]. For Jeju Island, Hamm et al. (2008) reported that the transmissivity was estimated based on specific capacities from time-drawdown data [40], and the hydraulic diffusivity was computed by using the tidal responses from time series data of the groundwater levels [41]. However, these studies did not consider the highly heterogeneous and complex multi-layered aquifer systems of Jeju Island, which have highly-permeable zones of hyaloclastite, sand/gravel beds, and clinkers [16]. Jeju Island has diverse geology in different areas and irregular aquifers of confined, phreatic, or leaky confined types, along with the presence of low-permeability layers (U-formation and the Seogwipo formation), since it was formed by volcanic activity over long timescales.

The bottom part of wells SS-1, SS-2, and SS-3 in the study area consist of the Seogwipo formation (SGF) and the U-formation (UF), which gradually become thicker from the coast to the center of Jeju Island (Figure 2). In well SS-1, a porous hyaloclastite layer overlies the SGF and porous pyroclastite, sand, and agglomerate layers intercalate between basalt layers. Low-permeability sediments like clay, silt, and silty sand can be found in the upper part of the basalt layers of well SS-1. In well SS-2, permeable pyroclastite is found in the upper part, and a cataclastic zone indicated by the dotted rectangle is also considered a permeable zone. Low-permeable clay and silt layers are located between the basalt layers. In well SS-3, permeable pyroclastite layers and low-permeable clay layers are repeated vertically between the basalt layers. A scoria/coarse-fragments layer, which is indicated by the dotted rectangle and is located in the upper part of well SS3, also acts as a permeable zone.

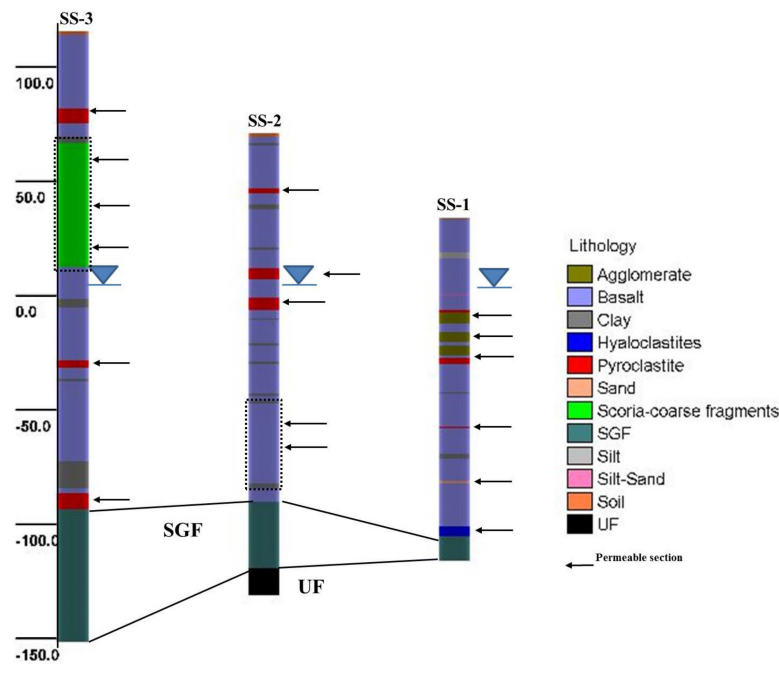


Figure 2. Lithology logs with the permeable sections in wells SS-1, SS-2, and SS-3.

The temperature and EC logs allowed us to identify the freshwater saltwater interface and permeable zones in the coastal multi-layered aquifers. Based on the EC and temperature logs from wells SS-1, SS-2, and SS-3, it is apparent that the groundwater level lies approximately at sea level and the transition zone becomes deeper as the distance from the coast increases (Figure 3). The temperatures in the transition zone are higher than those in the freshwater zone. The transition zone and the mixed zone of saltwater and freshwater also have variable salinity because of ocean tides and because of pressure differences between the freshwater and saltwater [32].

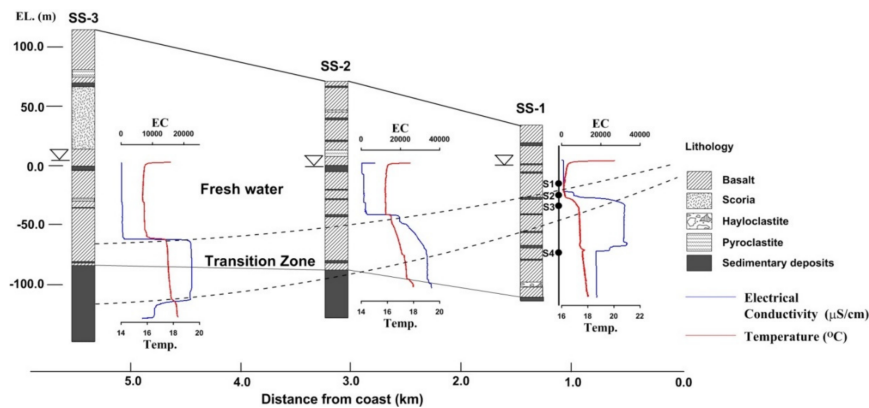


Figure 3. Lithology and groundwater temperature and electrical conductivity (EC) logs in the monitoring wells.

### 3. Methods

#### 3.1. Noise Removing Method

The original groundwater level data were corrected for atmospheric pressure changes and were filtered to remove the relatively low-frequency terms from the oceanic tides using the modified moving average method as follows.

$$X_t^* = X_t - \frac{X_{t-n} + \dots + X_t + \dots + X_{t+n}}{2n + 1} \tag{1}$$

where  $X_t^*$  is the filtered groundwater level,  $X_t$  is the original groundwater level corrected for atmospheric pressure, and  $n$  is the number of samples in the moving average before and after  $X_t$ . In this study, changes in groundwater level due to earthquakes were evaluated using  $n = 2$  in Equation (1).

### 3.2. Tidal Effect

An analytical solution for a single aquifer considering the storage coefficient together with the hydraulic diffusion coefficient and tidal effect can be used to estimate transmissivity in coastal aquifers. In this case, fluctuation in groundwater level is generated by pressure wave transmission from both earth and oceanic tides. Consequently, in coastal aquifers, the velocity, amplitude, wavelength, and attenuation of pressure waves are governed by the tidal frequency and amplitude, transmissivity, storage coefficient, and distance from the coast [42]. Groundwater level variation due to tidal changes is analogous to the heat transfer model [42–44]:

$$h(x, t) = h_{msl} + A \cdot \exp\left(-\sqrt{\frac{\omega S}{2T}}x\right) \cdot \sin\left(\omega t - \sqrt{\frac{\omega S}{2T}}x + c\right) \quad (2)$$

where  $h$  is the groundwater level (L),  $h_{msl}$  is the average sea level (L),  $A$  is the amplitude of the ocean tide (L),  $x$  is the distance from the coast (L),  $T$  is the transmissivity ( $L^2T^{-1}$ ),  $S$  is the storage coefficient (-),  $c$  is the phase shift (-), and  $\omega$  is the tidal speed ( $=2\pi/t_0$ ) with a tidal period  $t_0$  (T) and time  $t$  (T). According to Equation (2), the amplitude of the groundwater level,  $H_X$ , is:

$$H_X = h(x, t) - h_{msl} = H_0 \cdot \exp\left(-\sqrt{\frac{\omega S}{2T}}x\right) = H_0(-px) \quad (3)$$

where  $H_0$  is the amplitude of the ocean tide and  $p = \sqrt{\omega S / (2T)}$ .

The delay time of the groundwater level fluctuation,  $t_\tau$ , due to the tidal effect is:

$$t_\tau = \frac{xS}{2pT} \quad (4)$$

where  $t_\tau$  can be obtained by cross-correlation analysis between the ocean tides and the groundwater level. The  $t_\tau$  values for multiple aquifers that possess different oceanic tidal effects are estimated by using cross-correlation analysis between the oceanic tide and EC along the vertical profile. Equations (2)–(4) can be applied to both confined and unconfined aquifers when the ratio of the groundwater level fluctuation to the aquifer thickness is less than 0.02 for the unconfined aquifer [45].

## 4. Results

### 4.1. Groundwater Level Changes in the Study Area

After the 2011 M 9.0 Tohoku-Oki earthquake, a change in the groundwater level occurred at 14:51 at well SS-3 and at 14:52 at well SS-1 (Table 2, Figure 4). The tidal effect on the groundwater levels in the monitoring wells was considered after correction for atmospheric pressure. This tidal effect was found to diminish in accordance with the distance between the coast and the monitoring wells, with a large tidal effect at well SS-1 at a distance of 1.6 km, and a small tidal effect at well SS-3 at a distance of 5.4 km (Figure 4a). By eliminating both the oceanic and earth tidal effects (Figure 4b), the type of oscillation affecting the pure groundwater levels by the earthquake was verified (Figure 4c). Oscillatory changes in the groundwater levels at greater distances from the epicenter [46,47] are related to the permeability or transmissivity of aquifers as well as pore pressure changes and the inflow and outflow of water through wells in the aquifers [5,6,8,48].

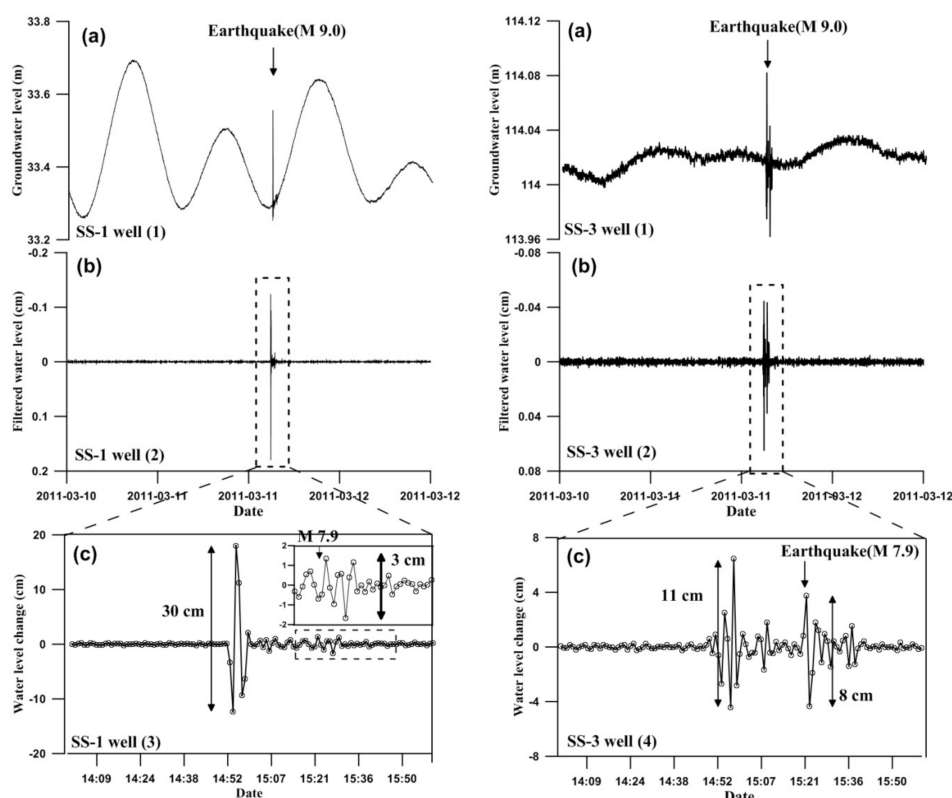


**Figure 4.** Changes in groundwater level caused by the M 9.0 Tohoku-Oki earthquake and the M 7.9 aftershock in wells SS-1 and SS-3.

**Table 2.** Groundwater level changes due to the 2011 M 9.0 Tohoku-Oki earthquake and its M 7.9 aftershock.

OW	Earthquake Magnitude (M)	Water Level Change (cm)	Response Pattern	Response Period (min)	Start Time (hh:mm)	End Time (hh:mm)
SS-1	9.0	30.4	Oscillation	37	14:52	15:09
	7.9	2.3	Oscillation			
SS-3	9.0	10.9	Oscillation	49	14:51	15:39
	7.9	8.1	Oscillation			

Response period: sum of M 9.0 + M 7.9.

In well SS-1, the change in groundwater level caused by the Tohoku-Oki earthquake was ~30 cm, with an initial water-level change accompanying the P wave and the maximum amplitude accompanying the Rayleigh wave. By contrast, at well SS-3, the groundwater level change was only ~11 cm, with a maximum amplitude accompanying the Rayleigh wave. By the time of the M 7.9 earthquake, wells SS-1 and SS-3 displayed water level changes of ~2.3 cm and ~8 cm, respectively, with oscillation-type water-level changes continuing from 14:52 until 15:29 (for ~37 min) at well SS-1 and from 14:51 until 15:39 (for ~49 min) at well SS-3 (Table 2). Well SS-1, located near the coast, only displayed a 0.3 m drawdown via the pumping of 1200 m<sup>3</sup>/day, whereas well SS-3 underwent a drawdown of ~1.6 m from ~1000 m<sup>3</sup>/day pumping (Table 2). Consequently, it was concluded that the difference in groundwater level changes due to the seismic waves at wells SS-1 and SS-3 were due to different hydraulic characteristics near the wells. In the study area, permeable structures that developed at depth act as conduits for groundwater flow and affect groundwater levels and pressure changes in aquifers when seismic waves pass through. Well SS-3 is ~100 m deeper than well SS-1 and demonstrates a longer stabilization time of water levels due to the relatively larger pressure change caused by the influence of seismic waves.

The hydraulic diffusivity ( $T/S$ ) of the monitoring wells was estimated using the relationship between ocean tide and groundwater level (Equations (3) and (4)): the  $T/S$  value for well SS-1 was  $2.61 \times 10^7 \text{ m}^2/\text{day}$  with  $x = 1600 \text{ m}$ ,  $H_0 = 0.85 \text{ m}$ ,  $H_x = 0.25 \text{ m}$ , and  $t_\tau = 4 \text{ h}$ ; the  $T/S$  value for well SS-3 was  $9.53 \times 10^8 \text{ m}^2 \text{ day}^{-1}$  with  $x = 5400 \text{ m}$ ,  $H_0 = 0.85 \text{ m}$ ,  $H_x = 0.024 \text{ m}$ , and  $t_\tau = 13 \text{ h}$ . Using general  $S$  values of  $10^{-3}$  to  $10^{-5}$  [49], the  $T$  values for well SS1 lie between 261 and 26,112  $\text{m}^2 \text{ day}^{-1}$  and the  $T$  values for well SS-3 range from 9533 to 953,307  $\text{m}^2 \text{ day}^{-1}$  (Table 3).

**Table 3.** Hydraulic parameters based on the relationship between the groundwater level and tidal effect.

OW	$H_0$ (m)	$H_x$ (m)	$t_\tau$ (h)	$x$ (m)	$T/S$ ( $\text{m}^2 \text{ day}^{-1}$ )	$T$ ( $\text{m}^2 \text{ day}^{-1}$ )	$S$ (-)
SS1	0.85	0.25	4	1600	$2.61 \times 10^7$	261–26,112	$10^{-3}$ – $10^{-5}$
SS3	0.85	0.024	13	5400	$9.53 \times 10^8$	9533–953,307	$10^{-3}$ – $10^{-5}$

The  $T$  values of the monitored wells were closely related to the groundwater level changes that occurred when seismic waves reached the object aquifers [14,15], revealing that the permeability of the monitoring wells increases linearly with peak ground seismic wave velocity in the range of 0.21–2.1 cm/s during a long-term observation of the effects from earth tides [12]. Well SS-3, with higher  $T/S$  and  $T$  values, showed an attenuation phenomenon due to the large energy of the M 9.0 earthquake, as well as the wider spatial influence of the earthquake, with a longer duration (~12 min) of water level fluctuations at well SS-3 than well SS-1. In other words, an instantaneous increase of the groundwater level at well SS-1 can be explained by the short-term compression and expansion of the aquifer with a relatively low  $T/S$  (Figure 5).

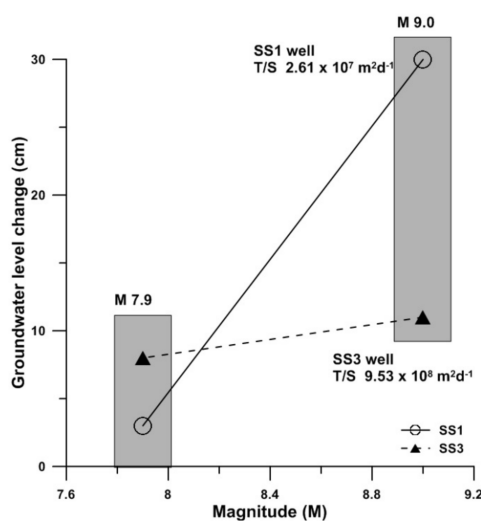


**Figure 5.** Groundwater level changes at wells SS-1 and SS-3 caused by the M 7.9 and M 9.0 earthquakes.

#### 4.2. Geophysical Well Loggings in Well SS-1

Using a geophysical well logging system (2000 m length winch and Micro loggerII produced by Robertson Geologging Co., United Kingdom), natural gamma, neutron, vertical flowmeter, EC, and temperature logs were carried out at a speed of 3 m/min with a measuring interval of 1 cm. Figure 6 is the result of this geophysical logging in well SS-1 before the M 9.0 Tohoku-Oki Earthquake [50]. The hydrogeological units of the lava flow sequences can be divided by using temperature or neutron logs [51,52]. The basalt formation until 135 m shows both high and low porosity because the outside of the basalt cooled rapidly and the inside of the basalt cooled slowly. The neutron log shows these properties. The intervals with very high porosity between the basalts are sedimentary formations. The formation below 135 m consists of tuff with relatively high porosity in well SS-1. From the natural gamma log, the basalt formation shows various values according to the components and the

sedimentary environment when the magma erupted. The tuff formation below 135 m shows high values of the natural gamma with the highest values found in the U formation below the tuff. Based on the logs, the temperature decreases from the top of the sequence downwards until the 60 m level, below which the temperature increases gradually along with the geothermal gradient. Based on the EC logs, the EC increases dramatically at around the 60 m level, caused by the effects of seawater intrusion at depths above the 80 m level.

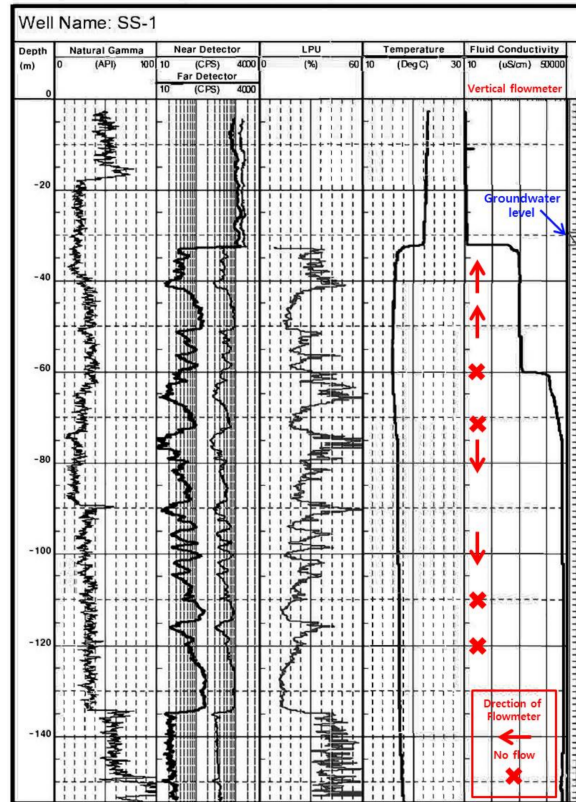


Figure 6. Results of the geophysical well logs from well SS-1 (from KIGAM (2004) report [50]).

#### 4.3. Vertical Profile of the Groundwater Temperature and the EC at Well SS-1

Changes in temperature and EC in well SS-1 occurred due to the seismic waves from the Tohoku-Oki earthquake. At well SS-1, the groundwater level was monitored at shallow depths, and the temperature and EC were measured at depths of 58 m (S1), 63 m (S2), 68 m (S3), and 111 m (S4) from the surface using a multi-depth system. The EC values at S1, S2, S3, and S4 are 1100–1600, 2000–30,000, 32,000–45,000, and 21,600–22,000  $\mu\text{S}/\text{cm}$ , respectively, depending on the ocean tidal effects and vertical lithology (Figure 7).

S1 is in the low salinity area, and the EC changes are only due to the up-down movement of water in the well. The high EC at high tide and the lower EC at low tide appears to increase vertically downwards. S2 is at the 60 m anomaly, and the EC front moves up and down at this depth (fresh, fresh-salty, and salty, 1000–30,000  $\mu\text{S}/\text{cm}$ ). This means that the EC front is more like that of Figure 2 than Figure 5 (i.e., a smoother front). S3 is below the 60 m front in an area where the EC decreases from about 10,000  $\mu\text{S}/\text{cm}$  over approximately 2 m. This means that either the EC log is not flat in that area, or that Figure 3 is very near the curve change observed in Figure 2. S4 is not near an EC front, so the vertical EC only changes by about 30  $\mu\text{S}/\text{cm}/2$  m (daily tide changes).

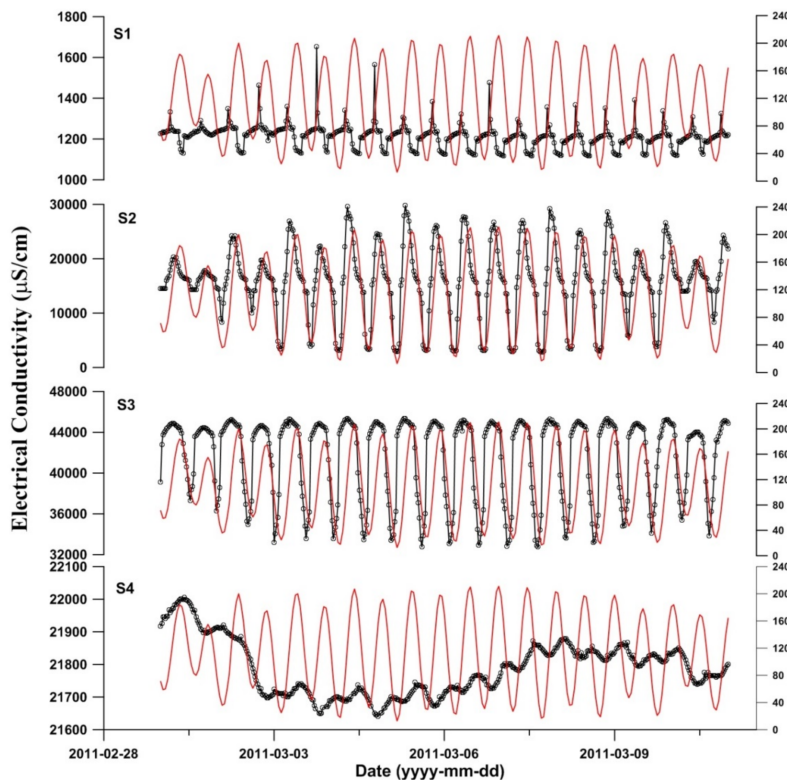


Figure 7. EC (black line) and ocean tide (red line) at S1, S2, S3, and S4 depths in well SS-1.

The tidal effects at the depths specified were estimated using cross-correlation analysis of EC vs. ocean tide data from the 10 days (1 March–10 March 2011) before the Tohoku-Oki earthquake. The delay times (correlations) of EC at the depths of S1, S2, S3, and S4 were 8 h (0.663), 11 h (0.803), 10 h (0.840), and 16 h (0.168), respectively (Figure 8), showing a higher correlation at the S2 and S3 depths, near the upper aquifer, and a lower correlation and longer delay time at the S4 depth, near the lower aquifer. Based on the data from well SS-1 (Figure 9), between the upper freshwater aquifer and the lower aquifer of the low-salinity aquifer, a zone of high-salinity water (>30,000  $\mu\text{S}/\text{cm}$ ) flows vertically downwards between the upper and lower aquifers.

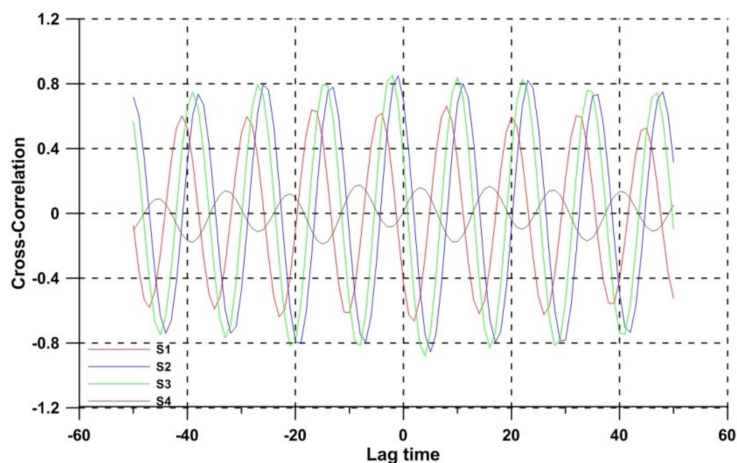


Figure 8. Cross-correlation of EC and ocean tide at S1, S2, S3, and S4 depths in well SS-1.

S1 seemed to show no change before or after the quake that was characterized with coseismic changes, suggesting that the water is stagnant in S1 (above 60 m). S2 showed only a very slight increase. The water column in the well moved upwards by a small distance, which may be consistent with a

temperature increase if S2 is below the surface at which the temperature has a significant influence. S3 might represent the water column in the well that appears to have moved slightly downwards (Figure 7). The EC values shifted from 33,000–44,000 (before) to 25,000–35,000 (after) with a gradient of ~10,000  $\mu\text{S}/\text{cm}$  over 2 m vertically downwards. S4 displayed a small EC gradient, demonstrating small tide-related variations in EC. EC then increased from 22,000 to 30,000  $\mu\text{S}/\text{cm}$  (Figure 9) and the temperature decreased after the quake (Figure 10).

After the Tohoku-Oki earthquake, EC changes at well SS-1 displayed various patterns at different depths. The EC values at the S1 depth rose instantaneously from 1200 to 3200  $\mu\text{S}/\text{cm}$  and gradually recovered to the original state. The EC values at the S2 depth increased from 17,000 to 33,000  $\mu\text{S}/\text{cm}$  during the tide effect and then gradually decreased over a longer time period relative to the other depths. By contrast, the EC values at the S3 depth instantaneously declined, rapidly reaching normal values, from 43,000 to 29,000  $\mu\text{S}/\text{cm}$ . This indicated freshwater inflow. At the S4 depth, the EC values progressively increased from 21,000 to 30,000  $\mu\text{S}/\text{cm}$  for a long time after the passage of the seismic waves, displaying a different tendency to that at the S3 depth (Table 4, Figure 9).

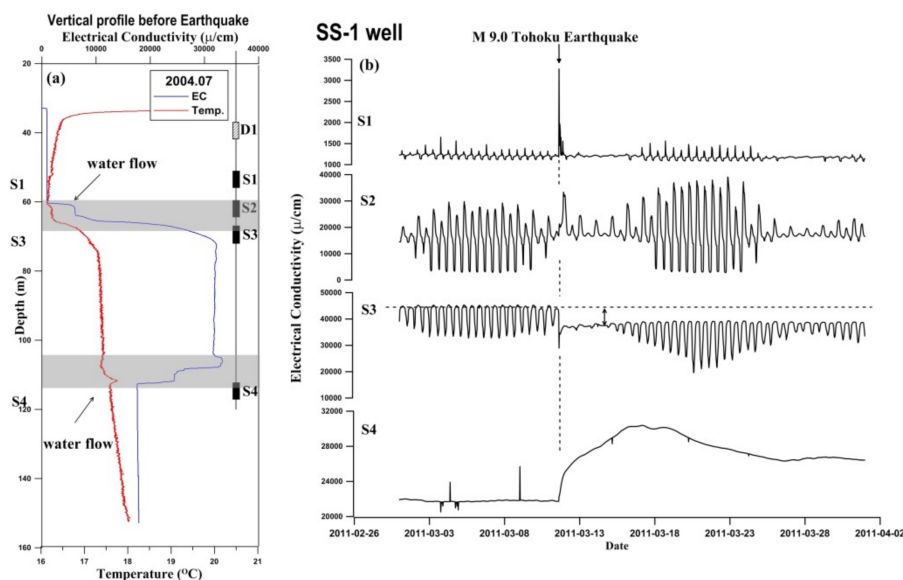
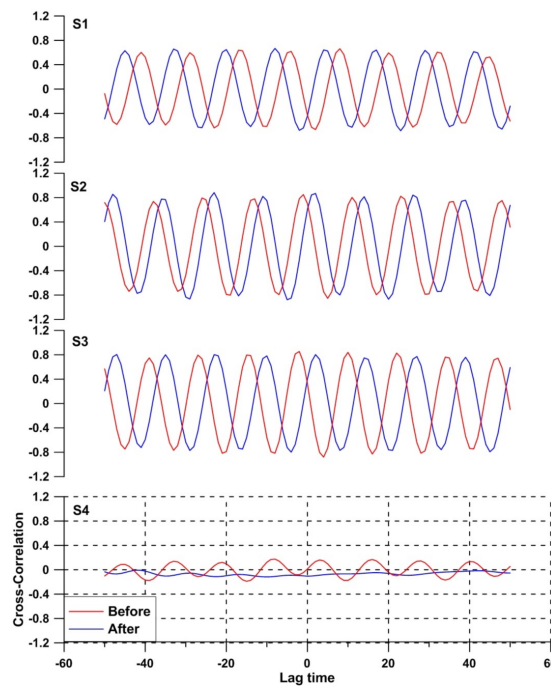


Figure 9. The EC responses by the earthquake at S1, S2, S3, and S4 depths in well SS-1.

Table 4. Electrical conductivity (EC) and temperature changes at S1, S2, S3, and S4 depths in well SS-1.

Well	Sensor	Depth (m)	EC ( $\mu\text{S}/\text{cm}$ )		Response Pattern	Temp. ( $^{\circ}\text{C}$ )		Response Pattern
			Before	After		Before	After	
SS-1	S1	58	1200	3200	Spike	-	-	None
	S2	63	17,000	33,000	Spike	16.6	16.9	Transient spike
	S3	68	43,000	29,000	Drop persistence	17.3	16.8	Drop persistence
	S4	111	21,000	30,000	Rise gradual	17.68	17.66	Drop gradual

According to the cross-correlation analysis, the delay times after the M 9.0 earthquake of EC and the ocean tide at depths of S1, S2, S3, and S4 took place at 4 h (0.643), 2 h (0.868), 2 h (0.804), and a negative value, respectively (Table 5, Figure 10). The delay time was reduced due to active groundwater flow induced by the earthquake, which produced the greatest influence near the S2 and S3 depths. Notably, after the earthquake, the response of the EC values with the ocean tide at the S4 depth was lower than in the upper sections, after which the EC values continuously increased due to saltwater inflow from the lower aquifer. Geophysical log data indicated active groundwater flow due to the influence of the earthquake near the bottom of the lower aquifer, even though only negligible groundwater flow normally occurred there as there is little effect from the ocean.



**Figure 10.** Cross-correlation of EC and ocean tide at S1, S2, S3, and S4 depths in well SS-1 before and after the M 9.0 earthquake.

**Table 5.** Cross-correlation and lag time of EC and ocean tide at S1, S2, S3, and S4 depths in well SS-1 before and after the M 9.0 Tohoku-Oki earthquake.

Well	Depth	(m)	Lag Time (h)		Cross-Correlation	
			Before	After	Before	After
SS-1	S1	(58)	8	4	0.663	0.643
	S2	(63)	11	2	0.803	0.868
	S3	(68)	10	2	0.840	0.804
	S4	(111)	16	17	0.168	−0.048

The temperature at each depth underwent only weak changes. At the S1 depth, a small peak in temperature change was observed during the decrease in EC. The S2 depth showed a similar temperature change to the change in EC. At the S3 depth, the temperature displayed an instantaneous change, after which the trend deviated from the normal pattern. The S4 depth showed a decreasing trend sometime after the Tohoku-Oki earthquake and recovered ~15 days after the earthquake (Figure 11).

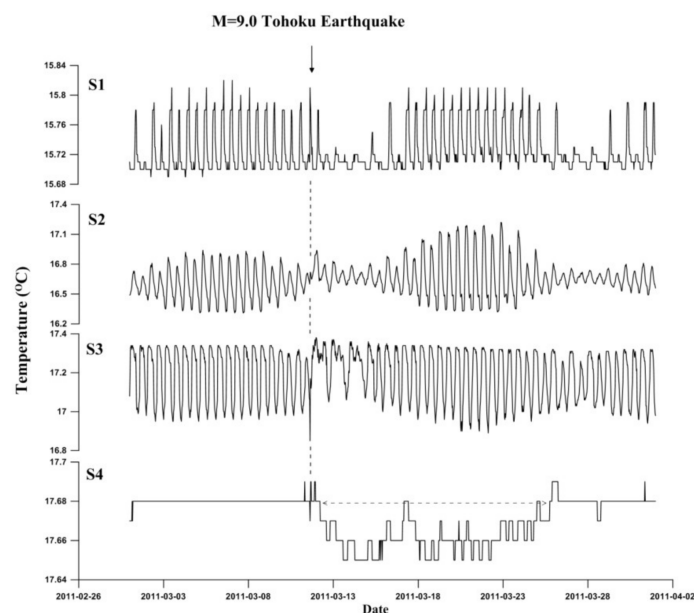


**Figure 11.** Vertical changes of the multi-layer temperature in the multi-depth detection system of well SS-1.

## 5. Discussion

Water pressure, temperature, and EC are usually measured at a single depth, with the advantage of easy measurement using a pressure transducer [15]. However, when seismic waves pass through coastal regions, measurement at a single depth is insufficient for detecting inflows and outflows of freshwater, as well as the saltwater inflow through wells in multi-layered aquifers. For instance, the S1 sensor of well SS-1 recorded groundwater level changes by the seismic waves but failed to detect water temperature changes as well as groundwater flow along the depth of the well.

Chemical changes in groundwater, with an increasing flow rate following incremental changes to permeability, have been proposed for pre-, co-, and post-seismic events both in the near-field and far-field from the epicenter (e.g., [53–55]). Changes in temperature or the EC of groundwater reflect groundwater movement when earthquakes or seismic waves pass through aquifers. In karstic aquifers, changes in EC are linked to the mixture of old and young groundwater following fluctuation influenced by seismic waves [28]. Chemical changes can also take place due to accelerated water-rock reactions following groundwater inflow from newly generated fractures or secondary pores [22] and to the switching or mixing of groundwater from new aquifers [22,24]. During the passing of seismic waves, temperature changes can also be generated by turbulence and the fluctuation of groundwater in wells [31] or by vertical mixing of the stratified water column in a reservoir [56].

In the study area, the well SS-1 site consists of upper and lower aquifers, as determined by the geophysical well logging, and seismic waves destroyed the equilibrium between the freshwater and saltwater in well SS-1 (Figure 12a). EC values at the S1 and S2 depths increased due to upward groundwater movement and turbulence in aquifer 1 due to the passing of seismic waves. The decrease of EC values at the S3 depth resulted from freshwater inflow from the aquifer existing between the S2 and S3 depths. The gradual increase of low EC values near the S4 depth reflects saltwater injection due to the seismic waves from aquifer 2. Since fresh- and saltwater flowed into well SS-1 from the upper and lower aquifers, the EC values of the S3 and S4 depths were maintained after the EC change (Figure 12b). The groundwater changes in well SS1 due to the Tohoku-Oki earthquake appeared to have been accompanied by various unexplained mechanisms. Nonetheless, the multi-depth monitoring system characterized the multi-layer aquifers through which groundwater freely moves when affected by earthquakes and seismic waves, overcoming the limitation of single-depth measurements.

The high-permeability zones could also be confirmed with vertical flowmeter logging (Figure 6). At well SS-1, an upward flow occurs at approximately 40 m depth of 1000  $\mu\text{S}/\text{cm}$ , and then a weak flow takes place in the transition zone. Records from a depth of 77 m in the saltwater zone recorded a downward flow, and the zone below 110 m showed a weak upward/downward flow. The result of the vertical flowmeter logging indicates that the groundwater from the aquifer at a depth of 40 m flows into the well and then mainly moves upwards, flowing into another aquifer. The saltwater flow at the 60–70 m zone produces a pressure difference with freshwater flowing downwards from the upper part, which continues moving downwards until it finally flows out of the lower part of the well.

The vertical flowmeter logs showed a similar result as the EC logs in well SS-1, helping to understand the influence of the earthquake on the groundwater flow in the multi-layered aquifer.

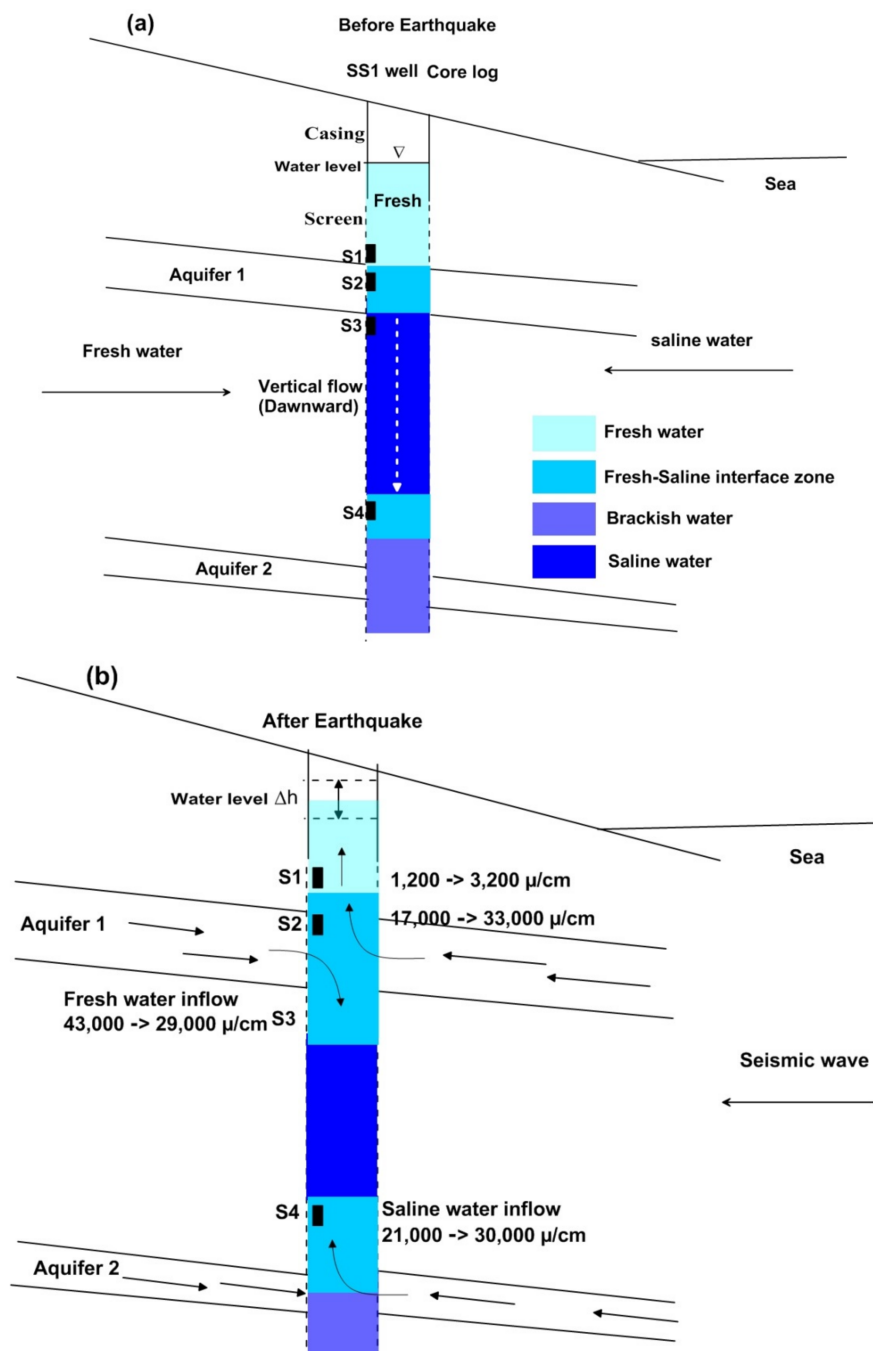


**Figure 12.** Conceptual model of the vertical EC changes caused by the Tohoku-Oki earthquake (before: (a) and after: (b)).

## 6. Conclusions

This study characterized changes in groundwater flow, EC, and temperature as groundwater level changes were recorded in monitoring wells in multi-layered coastal aquifers on Jeju Island caused by the 2011 M 9.0 Tohoku-Oki earthquake using a multi-depth monitoring system. This study identified that seismic waves produced changes in both groundwater flow and at the freshwater-saltwater interface in the multi-layered coastal aquifers. Single monitoring systems have often been used for detecting the effects of earthquakes or seismic waves but have failed to elucidate groundwater inflow/outflow and the precise flow along with depth in the monitoring wells. This study demonstrated that multi-depth monitoring systems can be effective tools to detect hydrogeological changes in multi-layered coastal aquifers caused by earthquakes or seismic waves and that they can be efficiently applied in other research on the relationship between earthquake and groundwater change.

**Author Contributions:** The idea of this was developed by S.-H.L. The text was mainly written by S.-H.L., B.W., and S.-Y.H. K.-Y.K., K.H., J.S., and S.H. collected and analyzed field data.

**Funding:** This study was financially supported by the 2018 Basic Research (19-3411) of the Korea Institute of Geoscience and Mineral Resources and the Korea Environment Industry & Technology Institute (KEITI) through the Subsurface Environment Management (SEM) Project, funded by the Korean Ministry of Environment (MOE) (2018002440004).

**Conflicts of Interest:** The authors declare no conflict of interest.

## References

1. Jonsson, S.; Segall, P.; Pedersen, R.; Bjornsson, G. Post-earthquake ground movements correlated to pore-pressure transients. *Nature* **2003**, *424*, 179–183. [[CrossRef](#)]
2. Wang, C.-Y.; Cheng, L.H.; Chin, C.V.; Yu, S.B. Coseismic hydrologic response of an alluvial fan to the 1999 Chi-Chi earthquake, Taiwan. *Geology* **2001**, *29*, 831–834. [[CrossRef](#)]
3. Koizumi, N.; Lai, W.-C.; Kitagawa, Y.; Matsumoto, Y. Comment on “Coseismic hydrological changes associated with dislocation of the September 21, 1999 Chichi earthquake, Taiwan” by Min Lee et al. *Geophys. Res. Lett.* **2004**, *31*, L13603. [[CrossRef](#)]
4. Petitta, M.; Mastrorillo, L.; Preziosi, E.; Banzato, F.; Barberio, M.D.; Billi, A.; Cambi, C.; De Luca, G.; Di Carlo, G.; Di Curzio, D.; et al. Water-table and discharge changes associated with the 2016–2017 seismic sequence in central Italy: Hydrogeological data and a conceptual model for fractured carbonate aquifers. *Hydrogeol. J.* **2018**, *26*, 1009–1026. [[CrossRef](#)]
5. Cooper, H.H.; Bredehoeft, J.D.; Papadopoulos, I.S.; Bennett, R.R. The response of well-aquifer systems to seismic wave. *J. Geophys. Res.* **1965**, *70*, 3915–3926. [[CrossRef](#)]
6. Liu, L.-B.; Roeloffs, E.; Zheng, X.-Y. Seismically induced water level fluctuations in the Wali well, Beijing, China. *J. Geophys. Res.* **1989**, *94*, 9453–9462. [[CrossRef](#)]
7. Brodsky, E.E.; Roeloffs, E.; Woodcock, D.; Gall, I.; Manga, M. A mechanism for sustained groundwater pressure changes induced by distant earthquakes. *J. Geophys. Res.* **2003**, *108*, 2390. [[CrossRef](#)]
8. Manga, M.; Wang, C.-Y. Earthquake hydrology. In *Treatise on Geophysics*; Schubert, G., Ed.; Elsevier Science: Amsterdam, The Netherlands, 2007; Volume 4, pp. 293–320. ISBN 978-0-444-51928-3.
9. Matsumoto, N. Regression-analysis for anomalous changes of groundwater level due to earthquakes. *Geophys. Res. Lett.* **1992**, *19*, 1193–1196. [[CrossRef](#)]
10. Muir-Wood, R.; King, G. Hydrological signature of earthquake strain. *J. Geophys. Res.* **1993**, *98*, 35–68. [[CrossRef](#)]
11. Roeloffs, E.A. Persistent water level changes in a well near Parkfield, California, due to local and distant earthquake. *J. Geophys. Res.* **1998**, *103*, 869–889. [[CrossRef](#)]
12. Elkhoury, J.E.; Brodsky, E.E.; Agnew, D.C. Seismic waves increase permeability. *Nature* **2006**, *441*, 1135–1138. [[CrossRef](#)]
13. Singh, V.S. Impact of the earthquake and Tsunami of December 26, 2004, on the groundwater regime at Neill Island (south Andaman). *J. Environ. Manag.* **2008**, *89*, 58–62. [[CrossRef](#)]
14. Wang, C.-Y.; Chia, Y.; Wang, P.-L.; Dreger, D. Role of S waves and Love waves in coseismic permeability enhancement. *Geophys. Res. Lett.* **2009**, *36*, L09404. [[CrossRef](#)]

15. Lee, S.-H.; Hamm, S.-Y.; Ha, K.C.; Ko, K.-S.; Cheong, J.-Y. Groundwater response analysis to multiple earthquakes on Jeju volcanic island. *Geosci. J.* **2012**, *16*, 469–478. [[CrossRef](#)]
16. Lee, S.-H.; Ha, K.C.; Hamm, S.-Y.; Ko, K.-S. Groundwater responses to the 2011 Tohoku Earthquake on Jeju Island, Korea. *Hydrol. Process.* **2013**, *27*, 1147–1157. [[CrossRef](#)]
17. Lachassagne, P.; Léonardi, V.; Vittecoq, B.; Henriot, A. Interpretation of the piezometric fluctuations and precursors associated with the November 29, 2007, magnitude 7.4 earthquake in Martinique (Lesser Antilles). *C. R. Geosci.* **2011**, *343*, 760–776. [[CrossRef](#)]
18. Wakita, H.; Igarashi, G.; Nakamura, Y.; Sano, Y.; Notsu, K. Coseismic radon changes in groundwater. *Geophys. Res. Lett.* **1989**, *16*, 417–420. [[CrossRef](#)]
19. Ma, Z.; Fu, Z.; Zhang, Y.; Wang, C.; Zhang, G.; Liu, D. *Earthquake Prediction: Nine Major Earthquakes in China (1966–1976)*; Springer: Berlin, Germany, 1990.
20. King, C.-Y.; Koizumi, N.; Kitagawa, Y. Hydrogeochemical anomalies and the 1995 Kobe earthquake. *Science* **1995**, *269*, 38–39. [[CrossRef](#)]
21. Kitagawa, Y.; Koizumi, N.; Tsukuda, T. Comparison of postseismic groundwater temperature changes with earthquake-induced volumetric strain release: Yudani hot spring, Japan. *Geophys. Res. Lett.* **1996**, *23*, 3147–3150. [[CrossRef](#)]
22. Claesson, L.; Skelton, A.; Graham, C.; Morth, M. The timescale and mechanisms of fault sealing and water-rock interaction after an earthquake. *Geofluids* **2007**, *7*, 427–440. [[CrossRef](#)]
23. Biagi, P.F.; Ermini, A.; Cozzi, E.; Khatkevich, Y.M.; Gordeev, E.I. Hydrogeochemical Precursors in Kamchatka (Russia) Related to the Strongest Earthquakes in 1988–1997. *Nat. Hazards* **2000**, *21*, 263–276. [[CrossRef](#)]
24. Claesson, L.; Skelton, A.; Graham, C.; Dietl, C.; Morth, M.; Torssander, P.; Kockum, I. Hydrogeochemical changes before and after a major earthquake. *Geology* **2004**, *32*, 641–644. [[CrossRef](#)]
25. Keskin, T.E. Groundwater changes in relation to seismic activity: A case study from Eskipazar (Karabuk, Turkey). *Hydrogeol. J.* **2010**, *18*, 1205–1218. [[CrossRef](#)]
26. Kitagawa, Y.; Koizumi, N. A study on the mechanism of coseismic groundwater changes: Interpretation by a groundwater model composed of multiple aquifers with different strain responses. *J. Geophys. Res.* **2000**, *105*, 19121–19134. [[CrossRef](#)]
27. Woith, H.; Wang, R.; Milkereit, C.; Zschau, J.; Maiwald, U.; Pekdeger, A. Heterogeneous response of hydrogeological systems to the Izmit and Duzce (Turkey) earthquakes of 1999. *Hydrogeol. J.* **2003**, *11*, 113–121. [[CrossRef](#)]
28. Charmoille, A.; Fabbri, O.; Mudry, J.; Guglielmi, Y.; Bertrand, C. Post-seismic permeability changes in a shallow fractured aquifer following a ML 5.1 earthquake (Fourbanne karst aquifer, Jura outermost thrust unit, eastern France). *Geophys. Res. Lett.* **2005**, *32*, L18406. [[CrossRef](#)]
29. Reddy, D.V.; Nagabhushanam, P. Groundwater electrical conductivity and soil radon gas monitoring for earthquake precursory studies in Koyna, India. *Appl. Geochem.* **2011**, *26*, 731–737. [[CrossRef](#)]
30. King, C.-Y.; Evans, W.C.; Presser, T.; Husk, R.H. Anomalous chemical changes in well and possible relation to earthquakes. *Geophys. Res. Lett.* **1981**, *8*, 425–428. [[CrossRef](#)]
31. Shi, Y.-L.; Cao, J.-L.; Ma, L.; Yin, B.-J. Tele-seismic coseismic well temperature changes and their interpretation. *Acta Seismol. Sin.* **2007**, *20*, 280–289. [[CrossRef](#)]
32. Bear, J.; Cheng, A.H.-D.; Sorek, S.; Quazar, D.; Herrea, I. *Sea-water Intrusion in Coastal Aquifer—Concepts, Methods and Practices*; Springer: Dordrecht, The Netherlands, 1999.
33. Anderson, M.P. Heat as a groundwater tracer. *Ground Water* **2005**, *43*, 951–968. [[CrossRef](#)]
34. Kim, K.-Y.; Chon, C.-M.; Park, K.-H.; Park, Y.-S.; Woo, N.-C. Multi-depth monitoring of electrical conductivity and temperature of groundwater at a multilayered coastal aquifer: Jeju Island, Korea. *Hydrol. Process.* **2008**, *22*, 3724–3733. [[CrossRef](#)]
35. Melloul, A.J.; Goldenberg, L.C. Monitoring of sea-water intrusion in coastal aquifers: Basics and local concerns. *J. Environ. Manag.* **1997**, *51*, 73–86. [[CrossRef](#)]
36. Park, N.-S.; Lee, Y.-D. Seawater intrusion due to groundwater developments in eastern and central Cheju watersheds. *J. Korea Soc. Groundw. Environ.* **1997**, *4*, 5–13.
37. Booh, S.A.; Jeong, G.C. Saline water intrusion into fresh groundwater aquifer of eastern area, the Cheju Island. *J. Eng. Geol.* **2000**, *10*, 115–130.
38. Kim, K.-Y.; Park, Y.-S.; Kim, G.-P.; Park, K.-H. Dynamic freshwater-saline water interaction in the coastal zone of Jeju Island, South Korea. *Hydrogeol. J.* **2009**, *17*, 617–629. [[CrossRef](#)]

39. Won, J.-H.; Lee, J.-Y.; Kim, J.-W.; Koh, G.-W. Groundwater occurrence on Jeju Island, Korea. *Hydrogeol. J.* **2005**, *14*, 532–547. [[CrossRef](#)]
40. Hamm, S.-Y.; Cheong, J.Y.; Jang, S.; Jung, C.Y.; Kim, B.S. Relationship between transmissivity and specific capacity in the volcanic aquifers of Jeju Island, Korea. *J. Hydrol.* **2005**, *310*, 111–121. [[CrossRef](#)]
41. Kim, K.-Y.; Shim, B.-O.; Park, K.-H.; Kim, T.H.; Seong, H.-J.; Park, Y.-S.; Koh, G.-W.; Woo, N.-C. Analysis of hydraulic gradient at coastal aquifers in eastern part of Jeju Island. *Econ. Environ. Geol.* **2005**, *38*, 79–89.
42. Ferris, J.G. Cyclic fluctuations of water level as a basis for determining aquifer transmissibility. *Int. Assoc. Sci. Hydrol.* **1951**, *33*, 148–155.
43. Jacob, C.E. Flow of groundwater. In *Engineering Hydraulics*; Rouse, H., Ed.; John Wiley and Sons Inc.: New York, NY, USA, 1950; pp. 321–386.
44. Werner, P.W.; Noren, D. Progressive waves in non-artesian aquifers. *Trans. Am. Geophys. Union* **1951**, *32*, 238–244. [[CrossRef](#)]
45. Roscoe Moss Company. *Handbook of Ground Water Development*; John Wiley & Sons: New York, NY, USA, 1990.
46. Blanchard, F.G.; Byerly, P. A study of a well gage as a seismograph. *Bull. Seismol. Soc. Am.* **1935**, *25*, 313–321.
47. Kano, Y.; Yanagidani, T. Broadband hydroseismograms observed by closed borehole wells in the Kamioka mine, central Japan: Response of pore pressure to seismic waves from 0.05 to 2 Hz. *J. Geophys. Res.* **2006**, *111*, B03410. [[CrossRef](#)]
48. Kunugi, T.; Fukao, Y.; Ohno, M. Underdamped responses of a well to nearby swarm earthquakes off the coast of Ito City, central Japan, 1995. *J. Geophys. Res.* **2000**, *105*, 7805–7818. [[CrossRef](#)]
49. Driscoll, F.G. *Groundwater and Wells*; Johnson Screens: St. Paul, MN, USA, 1986.
50. *Integrated Analysis of Groundwater Occurrence in Jeju*; Korea Institute of Geoscience and Mineral Resources (KIGAM): Daejeon, Korea, 2004. (In Korean)
51. Helm-Clark, C.M.; Rodgers, D.W.; Smith, R.P. Borehole geophysical techniques to define stratigraphy, alteration and aquifers in basalt. *J. Appl. Geophys.* **2004**, *55*, 3–38. [[CrossRef](#)]
52. Swanberg, C.A.; Walkey, W.C.; Combs, J. Core Hole Drilling and the “Rain Curtain” Phenomenon at Newberry Volcano, Oregon. *J. Geophys. Res.* **1988**, *93*, 10163–10173. [[CrossRef](#)]
53. Rojstaczer, S.; Wolf, S.; Michel, R. Permeability enhancement in the shallow crust as a cause of earthquake-induced hydrological changes. *Nature* **1995**, *373*, 237–239. [[CrossRef](#)]
54. Gaffet, S.; Guglielmi, Y.; Virieux, J.; Waysand, G.; Chawala, A.; Stolz, R.; Emblanch, C.; Auguste, M.; Boyer, D.; Cavaillou, A. Simultaneous seismic and magnetic measurements in Low-Noise Underground Laboratory (LSBB) of Rustrel, France, during the 2001 January Indian earthquake. *Geophys. J. Int.* **2003**, *155*, 981–990. [[CrossRef](#)]
55. Husen, S.; Taylor, R.; Smith, R.B.; Healsler, H. Changes in geyser eruption behavior and remotely triggered seismicity in Yellowstone Park produced by the 2002 M 7.9 Denali fault earthquake, Alaska. *Geology* **2004**, *32*, 537–540. [[CrossRef](#)]
56. Fuente, D.L.A.; Meruane, C.; Contreras, M.; Ulloa, H.; Nino, Y. Strong vertical mixing of deep water of a stratified reservoir during the Maule earthquake, central Chile (Mw 8.8). *Geophys. Res. Lett.* **2010**, *37*, L24608. [[CrossRef](#)]

